*International Journal of Robotics and Automation, Vol. 36, 2021*

*Special Issue: Automatic Detection and Assessment of Bridge Structures*

# DESIGN OPTIMIZATION OF STEEL TUBEWALL THICKNESS OF CONCRETE-FILLED STEEL TUBULAR ARCH BRIDGE

Lan Zhang* and Yao Xie**

## Abstract

As the main load-bearing component of a concrete-filled steel tubular arch bridge, the calculation of ultimate bearing capacity of arch ring is the key of structural design. The ultimate bearing capacity of a concrete-filled steel tube arch bridge is mainly related to hoop coefficient, initial stress of steel pipe and concrete shrinkage and creep. To optimize the design of a steel pipe wall thickness of arch bridge, a general relationship between section steel ratio and hoop coefficient, initial stress of steel pipe and concrete shrinkage and creep is derived. The design method of steel pipe wall thickness for a large-span concrete-filled steel tube arch bridge is proposed. A finite element model based on the Xianghuoyan Bridge is established. The research results show that the strength, stiffness, and stability of the bridge meet the requirements of the JTG/T D65-06-2015 standard when the steel pipe wall thickness is optimized. The design method can provide theoretical basis for the design of a large-span concrete-filled steel tube arch bridge in the future.

## Key Words

Concrete-filled steel tubular (CFST) arch bridge, wall thickness, steel ratio, optimization

## 1. Introduction

Concrete-filled steel tubular (CFST) arch bridges, in which the material characteristics of steel and concrete complement each other under stress, possess high bearing capacity [1]–[3]. The sectional steel ratio is a major design parameter for long-span CFST arch bridges and reflects the proportion between steel and concrete, which directly affects the bearing capacity of the structure. For a steel tube of a given diameter, the steel ratio is dependent solely on the wall thickness of the tube, which in turn is designed considering the confinement coefficient (*i.e.*, the reinforcement effect of the steel tube on the concrete), the initial stress in the tube, and the shrinkage and creep of the concrete [4]. However, few studies, mainly adopting finite element analysis (FEA) considering double nonlinearity, have focused on optimizing the wall thickness of the steel tube, and theoretical analyses are lacking, as evident from the later literature review.

The confinement coefficient indicates the reinforcement effect of steel tubes on concrete. Gu *et al.* [5] performed tests on CFST axial pressure short columns and discovered that the confinement effect increases as the wall thickness of the steel tube increases. Wu *et al.* [6] proposed the concept of a boundary confinement factor based on the unified strength theory. The bearing capacity and ductility of a CFST structure can be improved if the wall thickness satisfies this boundary confinement factor.

The process of building a CFST bridge induces an initial stress in the steel tube; Zhou *et al.* found that this stress decreases the bearing capacity of the bridge [7]–[11]. Through theoretical derivation and FEA, Zhao *et al.* [12]–[14] found that the lower the wall thickness of the steel tube is, the lower is the bearing capacity of the CFST arch bridge.

After construction, concrete creep leads to internal force redistribution in the CFST structure, affecting its ultimate bearing capacity [15]. According to Chen *et al.* [16]–[18], creep stress decreases as wall thickness increases.

Extant research on CFST structures has considered only one of the factors influencing ultimate bearing capacity, *i.e.*, confinement coefficient, initial stress in the steel tube, *or* concrete shrinkage and creep, and not the combined effects of these factors. To address this drawback, this study examines the optimal design and influence analysis of the wall thickness of the steel tube considering all three factors and determines the optimized wall thickness (range) under the influence of each factor, with the ultimate bearing capacity as the judgment index. To verify the optimized design equations, they were applied to the Xianghuoyan Bridge.

* School of Civil Engineering, Chongqing Jiaotong University, Chongqing, China; e-mail: zl_cqjtu@126.com

** Southwest Exploration and Design Institute of Nuclear Industry, Chengdu, China; e-mail: 2296921427@qq.com

Corresponding author: Lan Zhang

*Recommended by Dr. Jingzhou Xin*

*(DOI: 10.2316/J.2021.206-0539)*

## 2. Standards Governing the Wall Thickness of CFST Arch Bridge

In light of the large-scale construction of CFST arch bridges in China, the Ministry of Transport issued the "Specifications for Design of Highway Concrete-Filled Steel Tubular Arch Structures (JTG/T D65-06-2015)" standard, which stipulates that CFST structures should meet the following requirements:

1. The outer diameter of the steel tube should not be less than 300 mm and should not exceed 1,500 mm.
2. The main wall thickness of the main arch of the CFST should not be less than 10 mm.
3. The diameter–thickness ratio of the steel tube should not exceed 90 mm, and the diameter–thickness ratio of the coiled welded steel tube should not be less than 40 mm so as to avoid fabrication problems.
4. The steel ratio should be 0.04–0.20.

An analysis of more than 200 CFST arch bridges in China (Table 1) indicated that the steel ratio ranges between 5% and 12%.

## 3. Optimizing the Steel Tube Wall Thickness

Many factors affect the wall thickness of CFST structures. In this study, the effects of three such factors, namely, the confinement coefficient, initial stress, and concrete creep, on steel tube wall thickness are investigated.

The optimal wall thickness is one that maximizes the strength characteristics of both the steel tube and the concrete such that the CFST structure is optimally stressed. The bearing capacity of a section increases with increasing confinement coefficients. The initial stress generated in a section during the construction weakens its confinement effect and hence its bearing capacity; nevertheless, ensuring adequate wall thickness effectively limits the negative effects of the initial stress in the steel tube. The shrinkage and creep of concrete in the steel tube redistributes the stress, which differentially affects the wall thickness at different segments of the composite section.

For a CFST of a given diameter, wall thickness corresponds directly to the steel ratio. For ease of analysis, the steel ratio is used as a proxy to characterize the wall thickness of the steel tube.

### 3.1 Steel Ratio and the Confinement Effect of the Steel Tube

Under axial loading, the concrete in the steel tube experiences both axial and lateral deformation when the Poisson ratio of concrete ($\varepsilon_c$) is greater than that of steel ($\varepsilon_s$), *i.e.*, $\varepsilon_c > \varepsilon_s$. However, the steel tube prevents the lateral deformation of the concrete, which induces stress in the concrete; thus, this composite design substantially increases the bearing capacity of the structure [19]. This constraining effect of the steel tube is operationalized as the confinement coefficient or the constrained effect coefficient, $\xi$:

$$\xi = \frac{A_s f_y}{A_c f_{ck}} \tag{1}$$

where $f_y$ is the standard strength of steel, $f_{ck}$ is the standard compressive strength of the concrete axis, and $A_s$ and $A_c$ are the cross-sectional areas of the steel tube and concrete, respectively.

Table 1
Wall Characteristics of the Arch Rib Steel Tubes of Select CFST Arch Bridges in China

| Bridge Name | Arch Rib Section | Main Diameter ($D$, mm) | Main Wall Thickness ($t$, mm) | Diameter–Thickness Ratio ($D/t$) | Steel Ratio |
|---|---|---|---|---|---|
| Shitanxi Bridge | Four-limb truss | 550 | 8 | 68.75 | 0.061 |
| Fengjie Meixi River Bridge | Eight-limb truss | 920 | 14 | 65.71 | 0.064 |
| Fuxing Bridge | Four-limb truss | 950 | 24 | 39.58 | 0.109 |
| Nanning Yonghe Bridge | Four-limb truss | 1,220 | 16 | 76.25 | 0.055 |
| Maocaojie Bridge | Four-limb truss | 1,000 | 24 | 41.67 | 0.103 |
| Wushan Yangtze River Bridge | Four-limb truss | 1,220 | 22 | 55.45 | 0.076 |
| Nannidu Bridge | Four-limb truss | 920 | 14 | 65.71 | 0.064 |
| Bosideng Bridge | Four-limb truss | 1,320 | 30 | 44.00 | 0.098 |
| Zongxi River Bridge | Four-limb truss | 1,200 | 30 | 27.27 | 0.108 |
| Xiaohete Bridge | Six-limb truss | 1,100 | 28 | 39.29 | 0.110 |
| Yajisha Bridge | Six-limb truss | 750 | 20 | 37.50 | 0.116 |

In other words, the quantity of steel required is directly proportional to the confinement coefficient: the smaller (larger) the confinement coefficient is, the lower (greater) is the cross-sectional area of steel required.

#### *3.1.1 Relationship between Confinement Coefficient and Bearing Capacity*

Applying the limit equilibrium method, Cai [20] derived the equation for calculating the ultimate bearing capacity of CFST axially loaded short columns under certain assumptions, as follows:

$$N = A_c f_{ck}\left(1+\xi+\frac{3\sqrt{2}}{4}\sqrt{\xi}\right) \tag{2}$$

#### *3.1.2 Steel Ratio Considering the Effect of Confinement Coefficient on Ultimate Bearing Capacity*

$N_0$ represents the bearing capacity of a CFST when the confinement effect of the steel tube is not considered (*i.e.*, the nominal bearing capacity):

$$N_0 = f_{ck}A_c + f_y A_s \tag{3}$$

Accounting for the confinement effect improves the bearing capacity of the structure, which in turn depends on the steel ratio. The increase in bearing capacity can hence be expressed as follows:

$$\omega = \frac{N}{N_0} \tag{4}$$

Substituting (2) and (3) into (4),

$$\begin{aligned}\omega &= A_c f_{ck}\left(1+\xi+\frac{3\sqrt{2}}{4}\sqrt{\xi}\right)/\left(f_{ck}A_c + f_y A_s\right)\\ &= \left(1+\xi+\frac{3\sqrt{2}}{4}\sqrt{\xi}\right)/(1+\xi)\end{aligned} \tag{5}$$

Equation (5) is a $\xi$ function of the confinement coefficient:

$$\omega' = \frac{3}{8}\left(\sqrt{\frac{2}{\xi}}-\sqrt{2\xi}\right)/(1+\xi)^2 \tag{6}$$

if $\omega' = 0$, $\xi = 1$. Figure 1 shows the increase in bearing capacity as a function of the confinement coefficient. Evidently, the rate of increase in the bearing capacity of the steel tube is highest at $\omega_{\max} \approx 1.5$.

As $\xi = 1$,

$$\xi = \frac{A_s f_y}{A_c f_{ck}} = \frac{f_y}{f_{ck}}\alpha_s = 1 \tag{7}$$

$$\alpha_s = \frac{f_{ck}}{f_s} \tag{8}$$

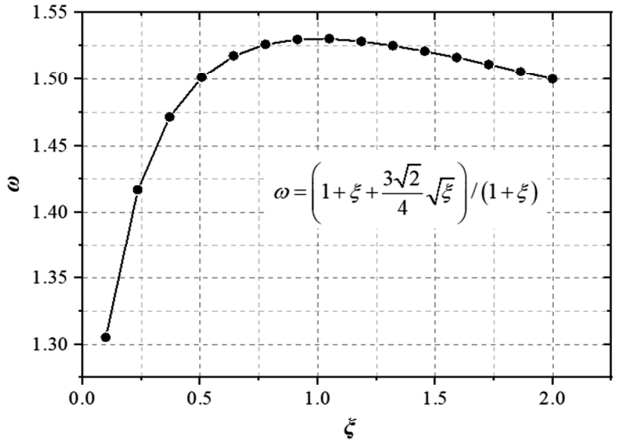


Figure 1. Rate of increase of the bearing capacity as a function of the confinement coefficient.

Equations (7) and (8) indicate that the intensity of steel and concrete directly affects the bearing capacity of the CFST structure. For a given steel ratio, when the increase in bearing capacity of the tube is the highest, the steel–concrete composite is fully optimized.

### 3.2 Steel Ratio and the Initial Stress in the Steel Tube

To build a CFST arch bridge, prefabricated hollow steel tubes and a cable system are used to form a bare arch, into which concrete is poured. Before the concrete sets, the steel tube bears its self-weight as well as the wet weight of the concrete; this generates initial stress and strain in the steel tube [21]. Here, the ratio of the initial stress $\sigma_0$ and the standard strength of the steel $f_y$ is called the initial stress coefficient $\beta$:

$$\beta = \frac{\sigma_0}{f_y} \tag{9}$$

The initial stress $\sigma_0$ and initial strain $\varepsilon_0$ affect the performance of the CFST composite member. Figure 2 reflects the relationship between the average stress and the strain of the concrete axial compression bar; $\sigma_0$ and $\varepsilon_0$ shorten the flexible working stage of the CFST and advances it into the elastoplastic working stage.

#### *3.2.1 Relationship between Initial Stress and Bearing Capacity*

Using the limit equilibrium method, Huang *et al.* [22] derived an equation to calculate the ultimate bearing capacity of axially loaded short columns under initial stress in a steel tube:

$$N_0 = A_c f_{ck}\left(1+\sqrt{1-\frac{3}{4}\gamma^2}\xi+\frac{3\sqrt{2}\gamma}{4}\sqrt{\xi}+\frac{\gamma}{2}\xi\right) \tag{10}$$

where $\gamma = \sqrt{1-\frac{3}{4}\beta^2}-\frac{1}{2}\beta$ and $\beta = \sigma_0/f_y$.

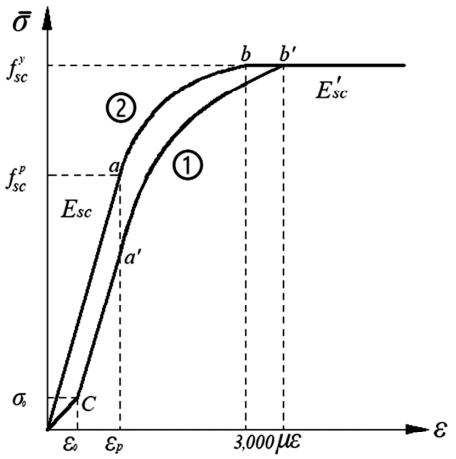


Figure 2. Effect of initial stress and strain on axial members.

Dividing (10) by (2) yields the following:

$$K_P = \frac{N_0}{N} = \frac{1 + \sqrt{1 - \frac{3}{4}\gamma^2}\xi + \frac{3\sqrt{2}\gamma}{4}\sqrt{\xi} + \frac{\gamma}{2}\xi}{1 + \xi + \frac{3\sqrt{2}}{4}\sqrt{\xi}} \tag{11}$$

where $K_p$ is the initial stress coefficient, and $N$ and $N_0$ are the ultimate bearing capacities of the axially loaded members in the presence and absence of initial stress, respectively.

### *3.2.2 Steel Ratio Considering the Effect of Initial Stress on Ultimate Bearing Capacity*

The initial stress coefficient $K_p$ reflects how the initial stress decreases the ultimate bearing capacity of the CFST structure. The smaller is the $K_p$, the stronger is the effect of the initial stress. Equation (11) expresses the relationship between initial stress in the steel tube, the confinement coefficient, and ultimate bearing capacity; this relationship also reflects the effect of initial stress on the confinement coefficient. Figure 3 depicts the foregoing relationship for the typical ranges of confinement coefficient (0.5–2.5) and selecting $\xi = 0.6$, 0.8, 1.0, 1.2, 1.4, 1.8, 2.2, 2.5, the degree of initial stress $\beta = 0 \sim 1$.

Evidently, initial stress and ultimate bearing capacity share a nonlinear relationship. The trends in the relationship between bearing capacity and initial stress are consistent under different confinement coefficients, but the coefficients of the corresponding bearing capacity differ depending on the confinement coefficient. For example, for $0.5 < \xi < 1.2$, the decrease in bearing capacity is not substantial. However, for $\xi > 1.2$, as the confinement coefficient increases, the ultimate bearing capacity of the CFST members decreases substantially even under the same initial stress.

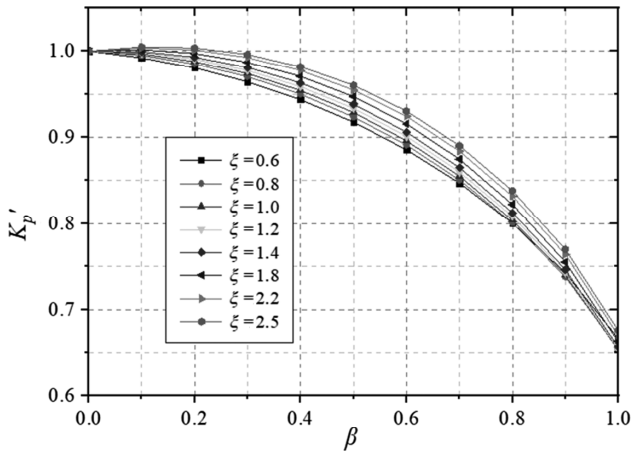


Figure 3. Relationship between $\xi$, $\beta$, and $K_p$.

Expanding (11),

$$K_p' = \frac{\frac{3\beta}{\sqrt{8\gamma+4\beta}+0.25} + \left(\frac{3\beta}{4\gamma+2\beta} + \frac{1}{2}\right)\cdot\sqrt{\xi} - \frac{9\xi\beta}{(4\gamma+2\beta+0.25)\cdot\gamma}}{4\,(1+3\gamma)\left(\xi + \sqrt{\xi} + 1\right)} \tag{12}$$

Here, for ease of calculation, consider $3\sqrt{2}/4 \approx 1.0$. Figure 4 depicts the relationship expressed in (12).

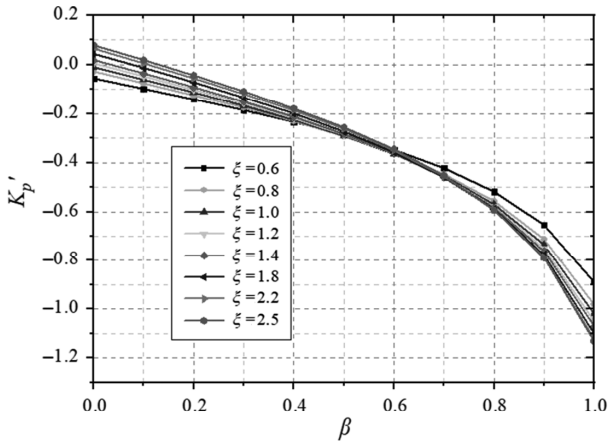


Figure 4. A plot of (12).

Figure 4 shows that for any confinement coefficient, when $\beta < 0.6$, the change in the initial stress coefficient is moderate, but beyond this limit, the effect of initial stress on the ultimate bearing capacity intensifies rapidly, and the ultimate bearing capacity decreases substantially.

In summary, the steel ratio of the CFST structure needs to be maintained such that the initial stress in the steel tube during construction does not exceed 0.6. For $\beta < 0.6$ and $\xi = 0.5$–1.2, the ultimate bearing capacity of the CFST structure does not decrease significantly, whereas for $\xi = 1.2$–2.5, this decrease is substantial. Therefore, to limit the initial stress,

$$0.5 < \xi < 1.2 \tag{13}$$

and

$$0.5\frac{f_{ck}}{f_y} < \alpha_s < 1.2\frac{f_{ck}}{f_y} \tag{14}$$

### 3.3 Steel Ratio and Concrete Creep Inside the Steel Tube

The concrete in the steel tube expands due to creep. Consequently, the additional concrete load is partially transferred to the sectional steel tube, increasing stress and strain in the tube. This phenomenon leads to stress redistribution in the composite section [12]. The concrete creep coefficient is

$$\phi'(t,t_0) = \frac{\phi(t,t_0)}{1+\dfrac{E_s}{E_c}[1+\rho\phi(t,t_0)]\alpha_s} \tag{15}$$

where $t_0$ is the concrete age under loading ($d$), $t$ is the concrete age under calculated ($d$), $\phi(t,t_0)$ is the concrete creep coefficient at loading age $t_0$ and concrete creep coefficient considering concrete age $t$ (see "Design specification of Highway Reinforced Concrete and Prestressed Concrete Bridges JTG D3362" for more details), $\alpha_s$ is the steel ratio, and $E_s$ and $E_a$ (MPa) represent the elastic modulus of steel and concrete, respectively.

Zhou [7] studied the effect of concrete creep in a filled steel tube under axial loading on structural stress and derived the stress redistribution equation for a CFST structure as follows:

$$\begin{cases} \Delta\sigma_s = \dfrac{n\cdot\sigma_0^c\cdot\phi(t,t_0)}{1+\alpha_s n[1+\rho(t,t_0)\,\phi(t,t_0)]} \\ \Delta\sigma_c = -\dfrac{\alpha_s n\cdot\sigma_0^c\cdot\phi(t,t_0)}{1+\alpha_s n[1+\rho(t,t_0)\,\phi(t,t_0)]} \end{cases} \tag{16}$$

where $n$ is the ratio of the elastic modulus of steel and core concrete, $n = E_s/E_c$, $\sigma_0^c$ is the initial stress in the concrete and the steel tube, $\sigma_0^c = \frac{F}{nA_s+A_c}$, $F$ is the axial loading, and $\rho(t,t_0)$ is the ageing coefficient.

Concrete creep induces additional stress in both the steel tube and the concrete, the magnitude of which depends on the steel ratio. Because $\sigma_0$ is affected by cross-sectional area of each material in a CFST section, deriving a relationship that exclusively considers the steel ratio $\xi$ is impossible. Therefore, two example CFST structures with different tube diameters and different axial loading are presented herein to discuss the relationship between the stress redistribution induced by creep and the steel ratio.

In both examples, $E_s = 2.06\times10^5$ MPa, $E_c = 3.45\times10^4$ MPa, $\phi(t,\infty) = 1.5$, $\rho(t,t_0) = 0.8$.

**Example 1.** Consider a steel tube with $D/t = 300/t$, axial loading $N = 600$ kN, and wall thickness of the steel tube = 5.0, 7.5, 10.0, 12.5, 15.0, 17.5, 20.0, 22.5, and 25.0 mm.

**Example 2.** Consider the tube of Xianghuoyan Bridge, which has $D/t = 1200/t$. The axial load is calculated using the perfusion scheme. The initial axial loading is $N = 12,537.8$ kN, and the wall thickness of the steel tube is 15.0, 17.5, 20.0, 22.5, 25.0, 27.5, 30.0, 32.5, and 35.0 mm.

Tables 2 and 3 show the calculated additional stress, and Figs. 5 and 6 illustrate the relationship between the steel ratio and creep-induced additional stress for Examples 1 and 2, respectively.

The previous tables and figures indicate that despite the differences in the dimensions of the steel tube, the relationship between steel ratio and creep stress redistribution is consistent. When the steel ratio is $\alpha_s \approx 0.1$, the curves of steel and concrete intersect, implying that the strengths of both materials are optimally traded off at this point. Hence, the optimized steel ratio considering the effect of concrete creep is $\alpha_s \approx 0.1$.

Table 2
Creep-Induced Additional Stress in Example 1

| Wall Thickness of Steel Tube (mm) | Steel Ratio | Steel Tube Stress (MPa) | Concrete Stress (MPa) | Standard Steel Tube Strength (%) | Standard Concrete Strength (%) |
|---|---|---|---|---|---|
| 15.0 | 0.070 | 29.8 | −2.1 | 8.65 | −5.9 |
| 17.5 | 0.108 | 23.7 | −2.6 | 6.87 | −7.2 |
| 20.0 | 0.148 | 19.5 | −2.9 | 5.65 | −8.1 |
| 22.5 | 0.190 | 16.4 | −3.1 | 4.75 | −8.8 |
| 25.0 | 0.235 | 14.0 | −3.3 | 4.07 | −9.3 |
| 27.5 | 0.282 | 12.2 | −3.4 | 3.54 | −9.7 |
| 30.0 | 0.331 | 10.7 | −3.5 | 3.10 | −10.0 |
| 32.5 | 0.384 | 9.5 | −3.6 | 2.75 | −10.3 |
| 35.0 | 0.440 | 8.5 | −3.7 | 2.45 | −10.5 |

Table 3
Creep-Induced Additional Stress in Example 2

| Wall Thickness of Steel Tube (mm) | Steel Ratio | Steel Tube Stress (MPa) | Concrete Stress (MPa) | Standard Steel Tube Strength (%) | Standard Concrete Strength (%) |
|---|---|---|---|---|---|
| 15.0 | 0.052 | 46.9 | −2.4 | 13.59 | 6.9 |
| 17.5 | 0.061 | 43.9 | −2.7 | 12.71 | 7.5 |
| 20.0 | 0.070 | 41.1 | −2.9 | 11.93 | 8.1 |
| 22.5 | 0.079 | 38.7 | −3.1 | 11.22 | 8.7 |
| 25.0 | 0.089 | 36.5 | −3.2 | 10.59 | 9.1 |
| 27.5 | 0.098 | 34.6 | −3.4 | 10.02 | 9.6 |
| 30.0 | 0.108 | 32.8 | −3.5 | 9.50 | 10.0 |
| 32.5 | 0.118 | 31.1 | −3.7 | 9.03 | 10.3 |
| 35.0 | 0.128 | 29.6 | −3.8 | 8.59 | 10.7 |

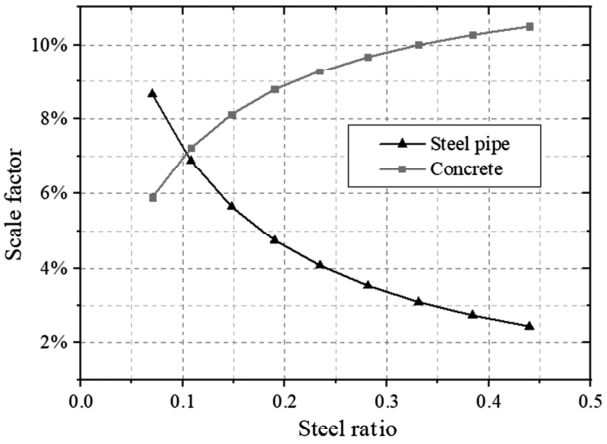


Figure 5. Relationship between steel ratio and creep-induced additional stress for Example 1.

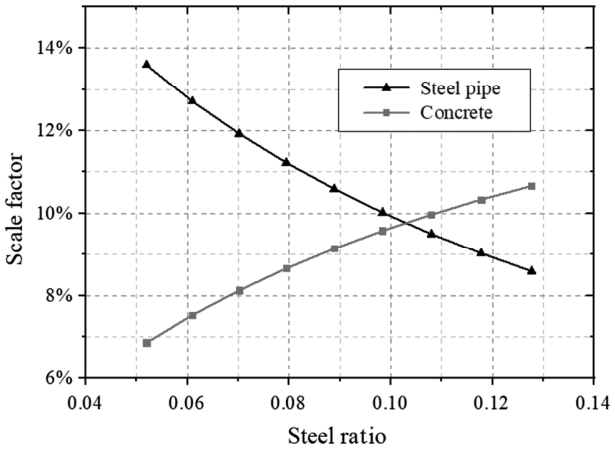


Figure 6. Relationship between steel ratio and creep-induced additional stress for Example 2.

## 4. Optimizing the Wall Thickness of the Xianghuoyan Bridge

### 4.1 Engineering Profile

The Xianghuoyan Bridge (Fig. 7) is a deck truss arch bridge with variable CFST sections. The main bridge has a net span of 300 m and a net vector height of 54.545 m (rise-to-span ratio = 1/5.5), with an arch axis coefficient m of 1.543 and net bridge deck width of 33.5 m. The main arch rib (Fig. 8) has sections of equal width but varying height. The section height of the arch foot and the vault is 9 and 5 m, respectively. The arch rib steel tube has sections of three wall thicknesses ($t = 26$, 28, and 35 mm; Fig. 9).

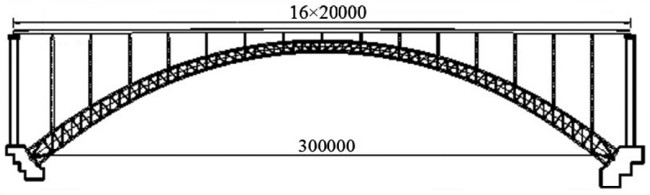


Figure 7. Cross section of the Xianghuoyan Bridge (unit: mm).

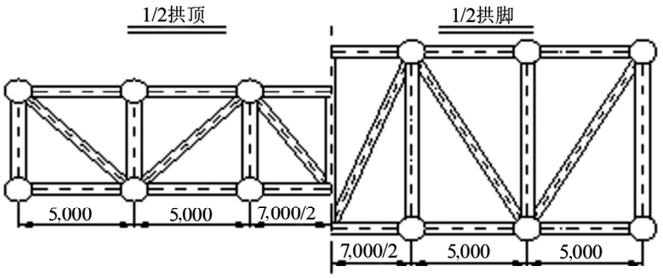


Figure 8. Cross section of the arch rib of the Xianghuoyan Bridge (unit: mm).

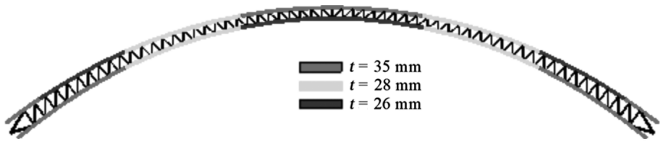


Figure 9. Wall thickness of the steel tube of the bridge.

Sections with the maximum wall thickness ($t = 35$ mm) are distributed mainly in the winding and lower strings of the arch foot, and the winding of the arch top; this is because these sections have relatively large bending moments. Sections with $t = 28$ mm are mainly distributed around the upper and lower chord of L/4. Sections with $t = 26$ mm are distributed between the upper chord arch foot and L/4 as well as the lower chord of the arch top.

### 4.2 Optimization Scheme

The steel ratios considering the effect of each factor analysed in this study (*i.e.*, the confinement coefficient, initial stress in the steel tube, and concrete creep) were optimized in the preceding sections. Applying the optimized equations to the Xianghuoyan Bridge, for a given tube diameter, the optimized wall thicknesses are as follows:

1. Steel ratio considering the effect of steel-tube confinement on core concrete:

$$\alpha_s = \frac{f_{ck}}{f_y} = \frac{35.5}{325} = 0.109$$

$$\alpha_s = \frac{A_s}{A_c} = \frac{4Dt - 4t^2}{D^2 - 4Dt + 4t^2} = 0.109$$

$$t \approx 30\,\text{mm}$$

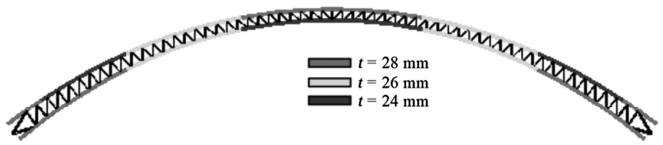


Figure 10. Optimized wall thickness of the steel tube of the bridge.

2. Steel ratio considering initial stress in the steel tube:

$$0.5\frac{f_{ck}}{f_y} < \alpha_s < 1.2\frac{f_{ck}}{f_y} \Rightarrow 0.051 < \alpha_s < 0.123$$

$$15.5 \le t \le 35.5$$

3. Steel ratio considering core concrete creep:

$$\alpha_s \approx 0.1 \Rightarrow t \approx 28\,\text{mm}$$

In summary, the optimized steel tube wall thickness of the Xianghuoyan Bridge is approximately 28 mm (Fig. 10), 2 mm thinner than the implemented design.

Table 4 lists the details of the main arch wall thickness before and after optimization. The optimized structure meets the requirements of the JTG/T D65-06-2015 standard.

### 4.3 Comparative Analysis of the Structural Strength, Stiffness, and Stability of the Main Arch

An arch bridge undergoes three key stages: erecting the arch using hollow steel tubes (the bare stage), filling the tubes with concrete (the concrete pouring stage), and the operation stage. In this section, we compare the strength, stiffness, and stability of the Xianghuoyan Bridge during these three stages against the standards.

1. Stress in the bare arch
   Tables 5 and 6 list the internal force, displacement, and stability of the bare arch before and after its optimization, respectively. In the tables, a negative sign indicates negative bending moment, compressive axial force, or downward displacement, as applicable. As is evident, the internal force, stiffness, and stability did not change significantly after the optimization.
2. Stress in the of main arch tube during the concrete pouring stage
   Figure 11 shows the stress in the steel tube and concrete in the main arch perfusion tube before and after optimization of the wall thickness.
3. Stress in the CFST arch rib during bridge operation
   Per the original design the maximum stress in the steel tube is 208 MPa, whereas the maximum stress

Table 4
Structural Characteristics before and after Optimizing the Thickness of the Main Arch Wall

| | Minimum Wall Thickness (mm) | Maximum Wall Thickness (mm) | Steel Ratio | Diameter–Thickness Ratio | Confinement Coefficient |
|---|---|---|---|---|---|
| Before optimization | 26 | 35 | 0.093–0.128 | 0.0217–0.0292 | 0.904–1.244 |
| After optimization | 24 | 28 | 0.085–0.100 | 0.0200–0.0233 | 0.826–0.972 |

Table 5
Internal Force, Displacement, and Stability in the Bare arch of the Xianghuoyan Bridge before Optimization

| Most Unfavourable Axial Force (kN) | | Least Favourable Bending Moment (kN m) | | Least Favourable Stress (MPa) | | Displacement (mm) | Stability Factor of Arch Rib Elasticity under Self-Weight |
|---|---|---|---|---|---|---|---|
| Magnitude | Location | Magnitude | Location | Magnitude | Location | | |
| −4,416.5 | Vault | 255.6 | Vault | −39.4 | Vault | −72.8 | 27.1 |
| −5,584.3 | Arch foot | −453.5 | Arch foot | −49.0 | Arch foot | | |

Table 6
Internal Force, Displacement, and Stability in the Bare Arch of the Xianghuoyan Bridge after Optimization

| Last Unfavourable Axial Force (kN) | | Least Favourable Bending Moment (kN m) | | Least Favourable Stress (MPa) | | Displacement (mm) | Stability Factor of Arch Rib Elasticity under Self-Weight |
|---|---|---|---|---|---|---|---|
| Magnitude | Location | Magnitude | Location | Magnitude | Location | | |
| −3,909.0 | Vault | 233.5 | Vault | −43.3 | Vault | −77.3 | 27.3 |
| −5,051.5 | Arch foot | −372.0 | Arch foot | −54.3 | Arch foot | | |

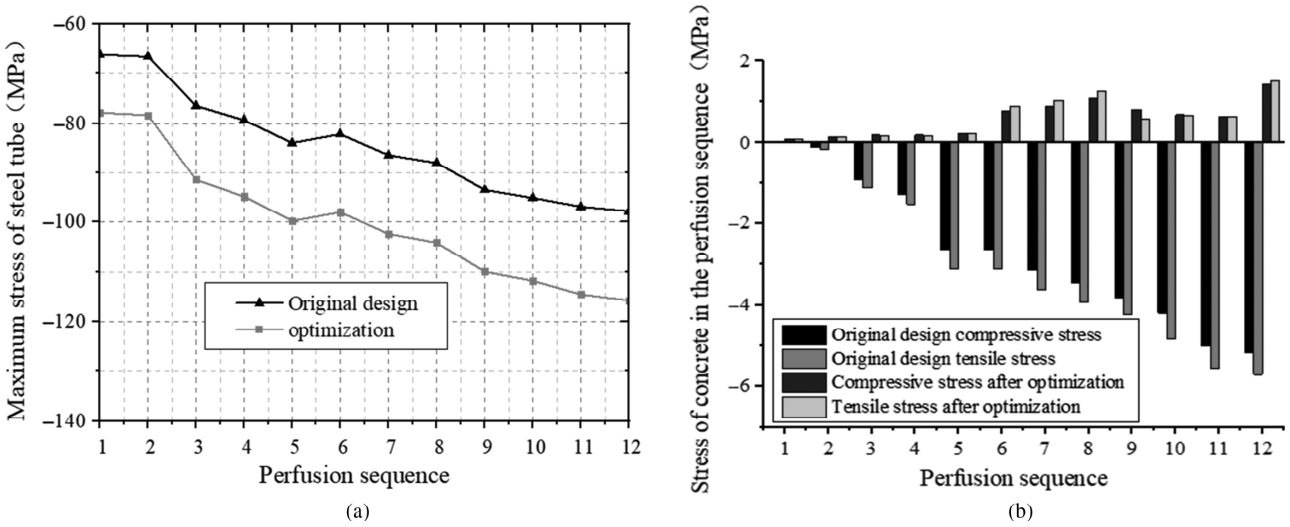


Figure 11. The maximum stress of the steel pipe in the pouring stage before and after optimization. Parts (a) and (b) represents the maximum tensile stress and maximum compressive stress of the concrete in the pipe before and after optimization.

Table 7
Overall Elastic Stability Coefficients of the Bridge before and after Optimization

| | Stage 1 | Stage 2 | Stage 3 | Stage 4 |
|---|---|---|---|---|
| Stability factor before optimization | 10.58 | 10.61 | 12.27 | 12.30 |
| Stability factor after optimization | 10.42 | 10.44 | 12.10 | 12.13 |

in the optimized steel tube is $222\,\text{MPa} < 325 \times 0.8 = 260\,\text{MPa}$, which meets the requirements of the standard.

4. Stability of the main arch

The overall elastic stability coefficient of the bridge did not change significantly after optimization and met the standard (>4) (Table 7).

Finally, before optimization, the stability coefficient considering double nonlinearity was 3.8, whereas that after optimization is 4.3, which too meets the requirements set in the standard.

## 5. Conclusion

The calculation of ultimate bearing capacity of main arch ring of the CFST arch bridge is the key of structural design. The value of wall thickness directly affects the ultimate bearing capacity of arch ring. Therefore, this article

discusses the influence of hoop coefficient, initial stress, concrete creep, and other factors on the wall thickness design of concrete filled steel tube structure. Based on the theoretical formula of ultimate bearing capacity derived by previous studies, the design method of steel pipe wall thickness of a large-span concrete-filled steel tube bridge is proposed by deducing further through function limit method and demonstration method. The specific conclusions are as follows:

1. the optimized steel ratio considering the confinement effect of steel tube is $\alpha_s = f_{ck}/f_y$;
2. the optimized steel ratio considering the initial stress in steel tube is $0.5 \times f_{ck}/f_y < \alpha_s < 1.2 \times f_{ck}/f_y$; and
3. the optimized steel ratio considering the creep of CFST is $\alpha_s \approx 0.1$.

## References


[1] Y.D. Li, C.R. Yao, and Y. Liang, A brief discussion on the progress and challenges of arch bridge technology, *Bridge Construction*, *42*(02), 2012, 13–20.

[2] J.L. Zheng, New trends in the development of long span concrete arch bridges in China, *Journal of Chongqing Jiaotong University (Natural Science Edition)*, *35*(S1), 2016, 8–11.

[3] B.C. Chen, J.G. Wei, J. Zhou, *et al.*, Application status and prospects of concrete-filled steel tubular arch bridges in China, *China Civil Engineering Journal*, *50*(06), 2017, 50–61.

[4] M. Ding, Y.D. Wang, C.H. Dai, *et al.*, Creep calculation and behavior analysis of concrete-filled steel tubular member under axial compression, *Engineering Mechanics*, *34*(06), 2017, 166–177.

[5] L.X. Gu, F.X. Ding, L. Fu, *et al.*, Research on the mechanical behavior of round-terminal concrete filled steel tubular columns, *China Journal of Highway and Transport*, *27*(01), 2014, 57–63.

[6] P. Wu, J.H. Zhao, C.G. Zhang, *et al.*, Boundary coefficient of concrete filled steel tubular columns with axial compression, *Journal of Architecture and Civil Engineering*, *31*(01), 2014, 83–89.

[7] S.X. Zhou, *Research on the influence of initial stress of steel tube on bearing capacity of CFST arch bridge*, MA, Chongqing University, Chongqing, China, 2007.

[8] S.X. Zhou, M. Zhang, and X.S. Wang, Nonlinear analysis of influence of initial stress of steel tube on bearing capacity of steel pipe arch bridge, *Chinese Journal of Computational Mechanics*, *27*(2), 2010, 291–297.

[9] F.Y. Huang, G. Yu, B.C. Chen, *et al.*, Experiment study on influence of initial stress in concrete filled steel tubular latticed columns under axial load, *Applied Mechanics & Materials*, *518*(11), 2014, 8.

[10] J.G. Wei, F.Y. Huang, and B.C. Chen, Research on the influence of initial stress to ultimate load carrying capacity of concrete filled steel tubular (single tube) arches, *Engineering Mechanics*, *27*(7), 2010, 103–112.

[11] H.L. Zhou, S.X. Zhou, X. He, *et al.*, Overview of the research on initial stress of concrete filled steel tube, *Highway Traffic Technology*, *6*, 2005, 58–61.

[12] Y. Li, J.H. Zhao, W.B. Liang, *et al.*, Ultimate bearing capacity of dumbbell – shaped CFST columns based on unified strength theory, *Industrial Construction*, *43*(5), 2013, 137–143.

[13] J.H. Zhao, W.Y. Feng, Y. Ling, *et al.*, Unified solution of ultimate bearing capacity of concrete filled square steel tubular columns considering initial stress, *Building Structure*, *4*, 2016, 56–61.

[14] B.W. Zhang, *Research on ultimate bearing capacity of CFST arch bridge considering initial stress and initial defect*, MA, Harbin Institute of Technology, Harbin, China, 2018.

[15] D.J. Zhang, S.M. Yi, and Y. Wang, Compressive behavior of concrete filled steel tubular columns subjected to long-term loading, *Thin-Walled Structures*, *89*, 2015, 205–211.

[16] B.C. Chen and X.Y. Lai, Shrinkage deformation of concrete filled steel tube and shrinkage stress of concrete filled steel tubular arches, *Journal of the China Railway Society*, *38*(02), 2016, 112–123.

[17] S.Y. Li, F.Q. Li, B.C. Chen, *et al.*, Analysis of the influence of creep on concrete-filled steel tubular arch bridges, *Journal of the China Railway Society*, *33*(3), 2011, 100–107.

[18] S.Y. Li, F.Q. Li, B.C. Chen, *et al.*, Analysis of the influence of creep on concrete-filled steel tubular arch bridges, *Journal of the China Railway Society*, *33*(03), 2011, 100–107.

[19] F.X. Ding and Z.W. Yu, Analysis of the mechanical mechanism of concrete steel tube short columns with round steel tube hoops, *China Railway Science*, *27*(06), 2006, 32–36.

[20] S.H. Cai, *Modern concrete filled steel tubular structure*, rev. ed. (Beijing: China Communications Press, 2007).

[21] L. Yan, J. Zhao, W. Liang, *et al.*, Unified solution of bearing capacity for concrete-filled steel tube column with initial stress under axial compression, *Tumu Jianzhu Yu Huanjing Gongcheng/journal of Civil Architectural & Environmental Engineering*, *35*(3), 2013, 63–69.

[22] F.Y. Huang, B.C. Chen, Y.Q. Lin, *et al.*, Research on the effect of initial stress on the ferrules of concrete-filled steel tubular columns, *Journal of Fuzhou University (Natural Science Edition)*, *39*(04), 2011, 575–580.


## Biographies

*Lan Zhang* was born in 1989. She received her master's degree in Bridge and Tunnel Engineering in 2015, and then worked in Chengdu Bridge Design Institute. She is currently studying for a doctorate degree in Bridge and Tunnel Engineering at Chongqing Jiaotong University. Her current research direction is the theoretical research of long-span concrete-filled steel tubular arch bridge.

*Yao Xie* was born in 1991. He received his master's degree in Architectural and Civil Engineering in 2017 and since then has been working in Chengdu Bridge Design Institute for Bridge Design. His current research direction is the theoretical research of long-span concretefilled steel tubular arch bridge.